www.vbripress.com/aml, DOI: 10.5185/amlett.2016.6067 Published online by the VBRI Press in 2016

Biosynthesis of silver nanoparticles using *Convolvulus pluricaulis* leaf extract and assessment of their catalytic, electrocatalytic and phenol remediation properties

Shadakshari Sandeep[1], Arehalli S. Santhosh[1], Ningappa Kumara Swamy[1, 2*], Gurukar S. Suresh[3], Jose S. Melo[4], Puttaswamappa Mallu[1]

[1]*Department of Chemistry, Sri Jayachamarajendra College of Engineering, Mysore 570006, India*
[2]*J. S. S. Research Foundation, SJCE Campus, Mysore 570006, India*
[3]*Department of Chemistry and Research Centre, N. M. K. R. V. College for Women, Bangalore 560011, India*
[4]*Nuclear Agriculture and Biotechnology Division, Bhabha Atomic Research Centre, Mumbai 400085, India*

[*]Corresponding author. Tel: (+91) 9741027970; E-mail: kumaryagati@gmail.com

Received: 20 July 2015, Revised: 16 October 2015 and Accepted: 24 March 2016

ABSTRACT

In the present work, we report on the biosynthesis of silver nanoparticles (AgNPs) using leaf extract of *Convolvulus pluricaulis* (Shankapushpi, bindweed) at room temperature. Synthesis of AgNPs is carried out by incubating the leaf extract in presence of $AgNO_3$. Formation of AgNPs is confirmed by the appearance of a prominent surface plasmon resonance band in the UV-visible spectrum at 420 nm. The biosynthesized AgNPs are characterized by powder X-ray diffraction (XRD) studies, Fourier-transform infrared spectroscopy (FTIR), scanning electron microscopy (SEM), transmission electron microscopy (TEM), thermo gravimetric analysis (TGA) and differential thermo gravimetric (DTG) analysis. Further, the biosynthesized AgNPs are investigated for their catalytic, electrocatalytic and phenol remediation properties. The investigations revealed that the biosynthesized AgNPs excel in their respective applications. Based on the results, present study concludes that AgNPs can be biosynthesized using leaf extract of *Convolvulus pluricaulis* and further can be employed for applications in electrochemical sensing, dye degradation and phenol remediation. Copyright © 2016 VBRI Press.

Keywords: Biosynthesis; electrocatalytic activity; phenol remediation; dye degradation.

Introduction

In the past few years, there have been numerous studies focusing on exploring properties of nanomaterials and their potential applications. Nanomaterials that have already been intensely explored include carbon nanotubes [**1**], fluorescent nanocrystals [**2**], nanoporous silica [**3**], dendrimers [**4**], liposomes [**5**], graphene [**6**] and nanoparticles [**7**]. Nanoparticles occur in different shapes such as spheres, platelets [**7, 8**], nanorods [**8, 9**], dimeric nanorods, hexagonal discs, P-shaped [**9**], U-shaped [**10**], nanoflowers [**11**] and nanobars [**12**]. Nano-sized organic and inorganic particles have been extensively studied and employed across the fields of photochemistry [**13**], electrochemistry as the element of batteries and super capacitors [**14, 15**], electrocatalysis [**16**] and the heterogeneous catalysis [**17**]. In recent years, metal and metal oxide nanoparticles based on silver, gold, copper, copper oxide, zinc oxide etc. have been applied in different fields such as medicine, pollution control, etc. [**18**].

Silver is particularly attractive for nanoscale electronics, antimicrobials, biosensing and imaging applications. Bulk silver has the highest thermal and electrical conductivity of any element making it a good candidate for usage as interconnects in electronic devices [**19, 20, 21**]. Nanosilver has been reviewed and reported to adsorb certain reactants onto its surface and effectively catalyzes reactions [**22**].

Most of the physicochemical methods used in the synthesis of nanoparticles are too expensive and also includes the use of toxic and hazardous chemicals that are responsible for the various environmental risks [**23**]. On the other hand, green synthesis of nanoparticles have been an interesting field as it is simple, cost effective and do not require any high pressure, temperature and toxic chemicals [**24, 25**]. Currently, microbes and plants are being exploited for the large scale synthesis of AgNPs. Biosynthesis using plant extract is preferred over that of microbes as the latter is more time consuming, require the use of nutrients to facilitate microbial growth and involve complex purification procedures [**22, 24, 25, 26**]. The extra-cellular synthesis of AgNPs by plants is also more useful over the chemical method that meets the requirements of industrial application such as biocompatibility and eco-friendliness [**27, 28**].

Convolvulus pluricaulis plant is a medicinal plant which has gained importance in traditional medicine due to its ability to treat a variety of medicinal conditions such as hypertension, neurodegenerative diseases, high blood

pressure, epilepsy, vomiting and diabetes. It is also known to improve memory and decrease cholesterol [**29**]. *Convolvulus pluricaulis* plant extract is a rich source of chemical constituents such as akaloids, phenolic/glycosides/triterpenoids/steroids [**30**] which helps in the reduction of metal salt to form the nanoparticles. *Convolvulus pluricaulis* plant is chosen for study as biosynthesized nanoparticles obtained from this plant are biocompatible and can be employed in applications treating above mentioned medical conditions.

The literature review shows lack of studies pertaining to electrocatalytic and phenol remediation behavior of biosynthesized AgNPs and it indicates the need for more studies in this direction. The present paper discusses the green synthesis of metallic AgNPs using leaf extract of *Convolvulus pluricaulis* and it investigates their possible utility in catalytic reduction of methyl orange (MO) dye, electrochemical sensing and in remediation of 2, 4-dichloropehnol (2, 4-DCP) from solution.

Materials and Methods

Chemicals

All the chemicals used in experiments are of analytical reagent grade purchased from Sigma Aldrich and Fischer Scientific.

Preparation of plant extract

Fresh leaves of *Convolvulus pluricaulis* plant are thoroughly washed in deionized water and shade dried. 10 g of plant leaves are crushed in 100 mL distilled water and filtered first through sterile muslin cloth and then through Whatman filter paper. The leaf extract is later used for synthesis.

Synthesis of AgNPs

10 mL of above leaf extract is mixed to 50 mL of an aqueous solution of 0.05 M $AgNO_3$ and incubated at room temperature until the solution color changed from pale yellow to dark brown. The formation of AgNPs is also monitored and confirmed by UV-visible spectroscopy. The formed AgNPs are centrifuged at 10,000 rpm for 15 min and purified using methanol. The repeated purification is done by giving several washes in methanol solution to remove the plant residues. AgNPs are finally dried at room temperature for evaporating methanol.

Characterization of AgNPs

The synthesized nanoparticles are characterized using UV-visible, FTIR, XRD, SEM, TEM, TGA and DTG methods.

UV - visible spectral analysis: The reduction of silver ions to AgNPs in the reaction mixture is confirmed by a visual color change from pale yellow to dark brown. The formation of AgNPs on reduction of silver ions is monitored by measuring UV-visible spectrum of the reaction mixture after diluting a small aliquot of the mixture with distilled water. The UV-visible spectral analysis is performed on Shimadzu-1800 UV-vis spectrometer using $AgNO_3$ solution free from leaf extract as control.

FTIR, SEM and TEM analysis: FTIR studies on the samples are carried out using Jasco FTIR 4100 (Japan) spectrometer. The spectral analysis is performed in the wave number range of 500-4000 cm^{-1}. SEM is performed on a ZEISS EVO40EP (Germany) microscope and the micrograph images of synthesized AgNPs are recorded. TEM is performed on JEOL/JEM 2100 microscope with an accelerating voltage of 200 kV and a resolution of 0.23 nm.

XRD measurements: The powder X-ray diffraction pattern of biosynthesized AgNPs is recorded using AXRD Bench-top Powder Diffractometer, Proto Manufacturing Limited. The XRD data is analyzed to determine the crystal structure and average crystal domain size of synthesized AgNPs.

TGA and DTG analysis: Thermo gravimetric analysis was performed using Q-500 TA Instruments (USA) and the thermograms are analyzed for thermal stability of synthesized nanoparticles. Differential thermo gravimetric analysis is also performed and the ash content, moisture content and organic component in synthesized nanomaterial are analyzed.

Application studies

Catalytic degradation of methyl orange dye: The catalytic activity of biosynthesized AgNPs is evaluated for the degradation of methyl orange dye by sodium borohydride ($NaBH_4$). For dye degradation experiments, a stock solution of 100 ppm methyl orange is used. A set of five 50 mL clean beakers are filled with 25 mL each methyl orange stock solution and then 1, 2, 3, 4 and 5 mg of biosynthesized AgNPs are mixed respectively by continuous stirring. 20 mg of $NaBH_4$ is mixed to each reaction mixture at 25 ^oC and the reaction is initiated. The progress of methyl orange degradation is monitored for 30 minutes by recording the absorption spectrum of the reaction mixture in regular intervals at λ_{max} = 465 nm using UV visible spectrophotometer. The percentage of methyl orange color degradation is calculated using the equation

$$C(\%) = \left(\frac{A_o - A_t}{A_o} \right) x100$$

where, A_0 = absorbance of undegraded methyl orange dye at time t = 0 sec, A_t = absorbance of degraded methyl orange dye at time t = t sec. Distilled water is used as control for measuring absorbance.

Electrocatalytic activity of AgNPs modified Gr electrode: A cylindrical graphite rod (Gr) having 6 mm diameter is inserted into a teflon holder of same internal diameter and electrical contact is established with a copper wire through the center of teflon bar. The electrode surface is polished with emery papers of different grades until a mirror shining surface is obtained. The Gr electrode is then sonicated, rinsed in milli-Q water and dried.

For adsorption of AgNPs on graphite electrode, a suspension of AgNPs in deionized water (w/v ratio of 10 mg in 1 mL) is prepared and drop casted onto the Gr surface. The resulting modified Gr electrode (Gr/AgNPs) is dried and stored until further usage.

The electrocatalytic behavior of bare Gr and modified Gr/AgNPs is investigated by cyclic voltammetry (CV) and electrochemical impedance spectroscopy (EIS) using Versa Stat 3 (Princeton Applied Research, USA). All electrochemical experiments are carried out in a three electrode cell with Gr/AgNPs as working electrode, standard calomel electrode (SCE) as reference electrode and platinum wire as auxiliary electrode. CV studies are carried out in the potential range of -0.2 V to +0.2 V Vs SCE at a scan rate of 50 mV/s in PBS solution (pH 7.0) using 5 mM $Fe(CN)_6^{3-/4-}$ as electrochemical probe. EIS is studied in the frequency range of 100 KHz to 10 Hz with an amplitude of 5 mV using 5 mM $Fe(CN)_6^{3-/4-}$.

Phenol remediation studies: For phenol remediation studies, a 250 ppm stock solution of 2, 4-dichlorophenol (2, 4 DCP) is used. 25 mL of 2, 4-DCP stock solution is taken in six different 50 mL Erlenmeyer's flasks and different quantities of biosynthesized AgNPs (10, 20, 30, 40 and 50 mg) are added to these flasks. The AgNPs are dispersed in 2, 4-DCP solution by constantly stirring for 30 minutes and later reaction mixture is left for 12 hours at room temperature. The reaction mixture is finally analyzed for phenolic content by 4-amino antipyrene method.

For the analysis of 2, 4-DCP in samples, 25 mL of sample is treated with 0.625 mL of NH_4OH (0.5N) solution and the pH was adjusted to 7.9±0.1 with phosphate buffer solution (PBS). About 0.25 mL of 4-amino antipyrine (4 %) and 0.25 mL of potassium ferricyanide (8 %) are added to above solution, mixed well and left for 15 minutes. The absorbance is measured at 500 nm after 15 minutes and the residual 2, 4-DCP concentration is determined from standard curve. The standard curve is prepared using a series of standard 2, 4-DCP solutions.

Results and discussion

Synthesis of AgNPs

For the synthesis of AgNPs, aqueous solution of $AgNO_3$ is mixed with leaf extract of *Convolvulus pluricaulis* and incubated at room temperature. The reaction mixture is initially pale yellow which gradually turned to dark brown. The visible color change from pale yellow to dark brown suggests the formation of AgNPs through reduction of Ag^+ ions to Ag^0 by the leaf extract (**Fig. 1A**, inset). The pure $AgNO_3$ solution and leaf extract have not shown any visible color changes during the same incubation period under similar conditions. The formation of AgNPs is further confirmed from UV-visible spectral studies.

UV-visible spectral studies

UV-visible spectroscopy is used as a tool to ascertain the formation of AgNPs. The UV-visible spectral measurements of reaction mixture at regular intervals during incubation period showed a gradual increase in absorbance. The absorbance reached a maximum and almost stabilized after 10 hours of incubation indicating the completion of reduction of silver ions to AgNPs. Further, a strong and broad peak in spectrum at 420 nm clearly confirmed the formation of AgNPs (**Fig. 1A**).

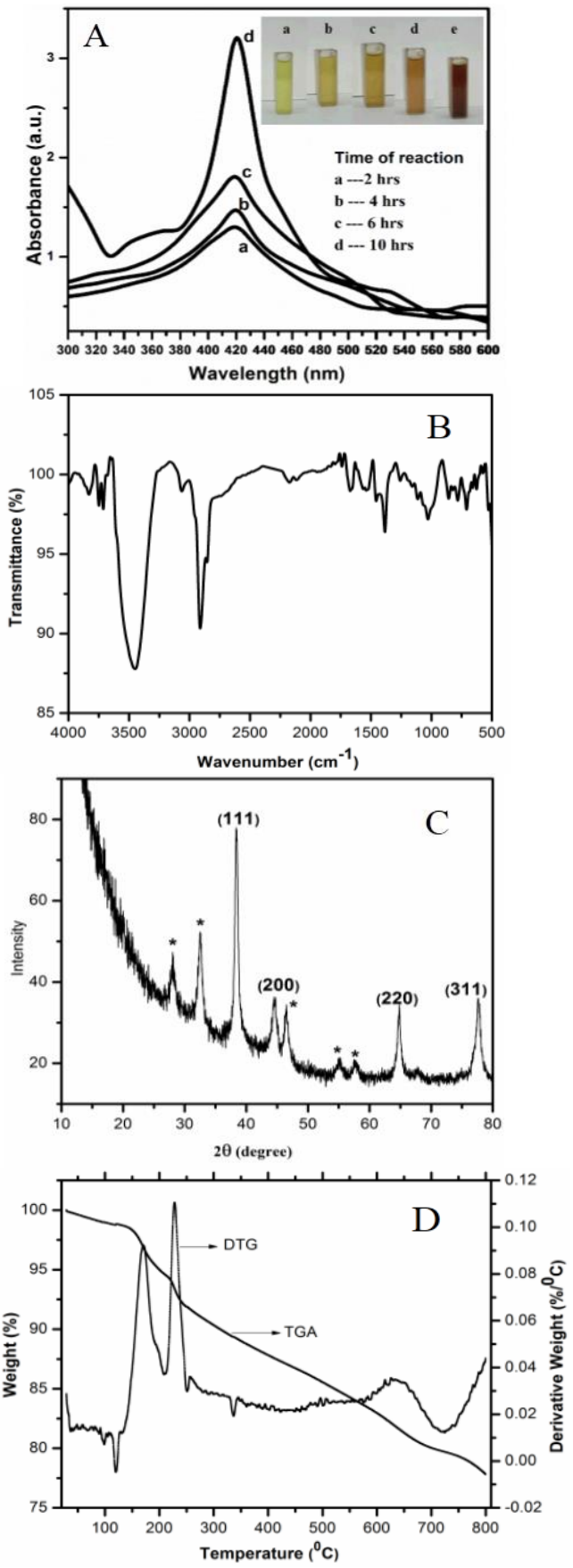

Fig. 1. UV-Vis spectra, inset picture shows the color reaction mixture at different time intervals of reaction (A), FTIR spectra (B), X-ray diffraction pattern (C), and TGA and DTG curves of biosynthesized silver nanoparticles (D).

This peak may be attributed to surface plasmon resonance in AgNPs [**26**]. UV-visible study clearly confirms completion of reduction of Ag^+ and formation of AgNPs in nearly 10 hours. The inset **Fig. 1A** shows the visible color change in reaction mixture at different time intervals of formation of AgNPs.

FTIR spectroscopic studies

The phytochemical and spectral studies reported in literature have established the presence of alkaloids, glucosides, carbohydrates, flavonoids, proteins, steroids, gums and mucilages in the plant extracts of *Convolvulus pluricaulis* and also in other *Convolvulus* species [**30, 31**]. In the present work, FTIR spectral study of biosynthesized AgNPs is carried out to establish the identity of biomolecules attached to AgNPs surface and their possible involvement in bioreduction of Ag^+ to Ag^0.

FTIR spectra of biosynthesized AgNPs showed prominent peaks at 3450, 2912, 1740, 1672, 1540, 1457, 1384, 1028 and 782 cm^{-1} (**Fig. 1B**). The most prominent and broad peak around 3450 cm^{-1} represent the –OH stretching vibrations corresponding to glycosides. The peaks at 2912 and 1457 cm^{-1} are possibly due to –C-H stretching and asymmetric bending vibrations of $–CH_3$ group respectively. The presence of amide group (-NH-CO-) of protein and the aromatic ring structures is revealed by the peaks around 1672 and 1540 cm^{-1} which corresponds to –C=C stretching vibrations in rings. The -C=O stretching vibration of –COOH group is revealed by peak around 1740 cm^{-1}. The signals positioned at 1384 and 1028 cm^{-1} indicate the in plane bending vibrations of –OH and C-O-C groups respectively. The aliphatic –C-H bending vibration has appeared as a signal at 782 cm^{-1}. The FTIR spectral analysis clearly suggests the presence of biomolecules with functional groups such as –OH, -C=O, -NH-CO-, -COOH, C-O-C, etc. as attachments to AgNPs surface and these biomolecules are possibly involved in reduction of Ag^+ to Ag^0.

XRD studies

The crystalline nature of synthesized AgNPs is confirmed by XRD. Powder XRD spectral pattern of AgNPs is shown in **Fig. 1C**. XRD spectrograph showed four intense peaks in the whole range of 2θ from 10^0 to 80^0. The peaks at 38.36, 44.54, 64.76 and 77.6 are indexed to be lattice planes with miller indices (111), (200), (220) and (311) respectively of AgNPs. The other peaks in XRD spectrum are possibly contributed by impurities and residues in plant extract. The crystal domain size (D) is calculated from the width of XRD peaks using Scherrer's formula

$$D = \frac{0.94\lambda}{\beta Cos\theta}$$

where, D is the average crystal domain size perpendicular to reflecting planes, λ is wavelength of X-rays used, θ is diffraction angle and β is full width half maximum (FWHM). The β values are corrected to eliminate error due to instrumental broadening of peaks using FWHM value from large grained silicon.

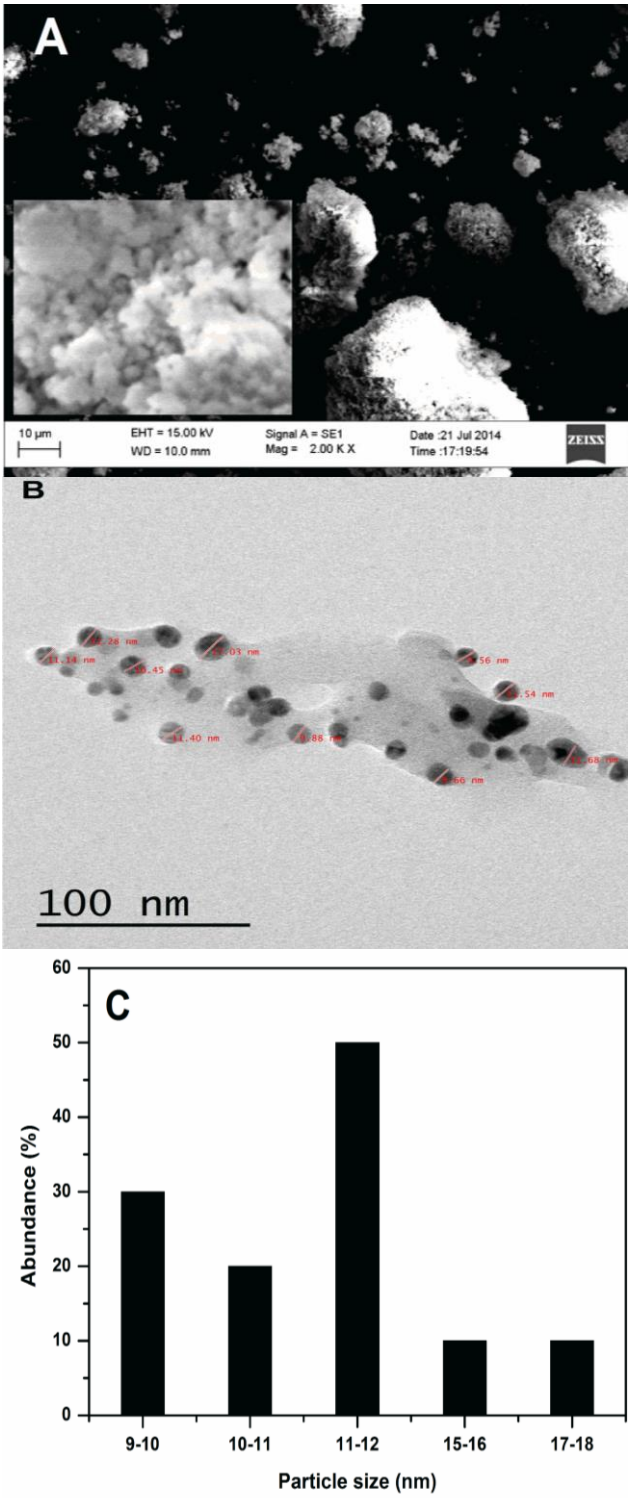

Fig. 2. SEM image of silver nanoparticle (A) inset shows the high resolution image (1µm), TEM image of silver nanoparticle (B), histogram obtained from TEM studies (C).

$$\beta_{corrected} = \sqrt{(FWHM)^2_{sample} - (FWHM)^2_{silicon}}$$

The calculated average particle size of nanoparticle is 19.62 nm. Various crystalline characteristics of biosynthesized AgNPs calculated from XRD data are shown in **Table 1**.

Table 1. XRD parameters of biosynthesized AgNPs.

S. no	2θ° (degree)	FWHM	Miller indices (hkl)	d_{hkl}	Crystal domain size D (nm)	Average domain size (nm)
1	38.36	0.5590	(111)	2.344	15.7	
2	44.54	0.8540	(200)	2.032	10.4	19.62
3	64.76	0.6790	(220)	1.438	14.4	
4	77.60	0.2796	(311)	1.421	38.0	

Thermal analysis

TGA and DTG analysis have been performed to analyze the purity and thermal stability of biosynthesized AgNPs. TGA data (**Fig. 1D**) indicates a very high thermal stability for AgNPs up-to a temperature of 200 ^{0}C. Thermal analysis data till 800 ^{0}C showed an ash content of 78 %, organic content of 21 % and moisture content of 1 %. The observed net weight loss of 22 % is attributed to organic content and moisture. DTG shows the presence of three thermally less stable organic components which further support high ash content recorded in TGA and presence of functional groups of organic molecules in FTIR data. The organic content may be organic residues or moieties of leaf extract attached to AgNPs surface even after washing with methanol. The thermogram shows 78 % ash content which is a product of oxidation of AgNPs to silver oxide (Ag_2O). The high ash content indicates the extent of purity of biosynthesized AgNPs. Thermal analysis clearly suggests that the synthesized AgNPs are thermally very stable and have considerable purity.

SEM and TEM analysis of AgNPs

The surface morphology of biosynthesized AgNPs are studied using SEM and TEM techniques. **Fig. 2A** shows SEM image of AgNPs. The SEM image reveals that the size of synthesized AgNPs is in the range of 10-40 nm. However, the nanoparticles tend to agglomerate to form still bigger structures. TEM study indicates that most of the nanoparticles are spherical in shape with varying sizes (**Fig. 2B**). The size distribution of AgNPs shown in histogram in **Fig. 2C** suggest that most particles have a size distribution around 11-12 nm.

Table 2. Percent degradation of MO dyes in presence of AgNPs in 30 minutes time.

S. No	Volume of MO used (mL)	Amount of $NaHB_4$ added (mg)	Amount of AgNPs added (mg)	Dye degradation (%)
1	25.0	20.0	0	03.35
2	25.0	20.0	1.0	92.03
3	25.0	20.0	2.0	95.20
4	25.0	20.0	3.0	96.44
5	25.0	20.0	4.0	97.36
6	25.0	20.0	5.0	97.72
7	25.0	0.0	5.0	00.00

Applications of AgNPs

Catalytic degradation of methyl orange dye

Degradation of MO by $NaBH_4$ is investigated both in presence and absence of biosynthesized AgNPs. The blank experiments performed without AgNPs showed nearly no change in absorbance for MO dye solution at its λ_{max}= 465 nm, indicating a very slow reduction rate for the reaction. The recorded degradation of dye in 30 minutes is only 3.35 %. However, on repetition of the same experiments in presence of AgNPs, there has been an immediate decrease in absorbance in a matter of 5-10 minutes indicating that MO is reduced effectively by $NaBH_4$ in the presence of AgNPs (**Fig. 3A, B**). The calculated values of percent degradation of MO in 30 minutes are shown in **Table 2**.

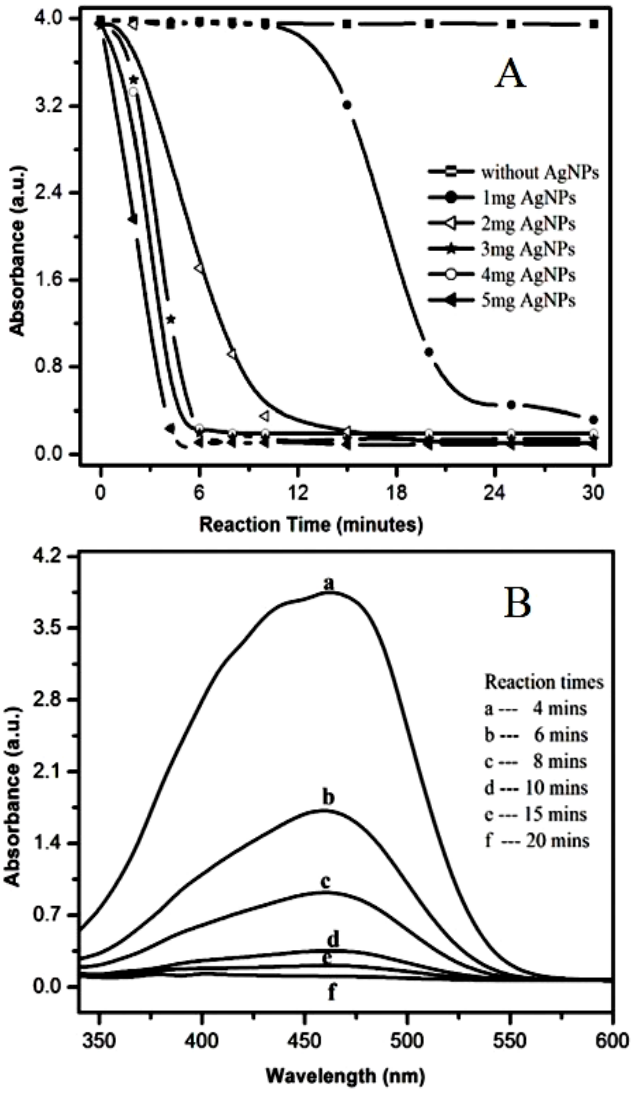

Fig. 3. Degradation of methyl orange dye by $NaBH_4$ at different concentrations of AgNPs (A) and UV visible spectra of reaction mixture (25ml MO + 20mg $NaBH_4$ + 2mg AgNPs) at different reaction times (B).

The degradation of MO reached a maximum in less than 10 minutes for almost all concentrations of AgNPs applied except for the concentrations of 1.0 mg where degradation has been relatively slower. The dye degradation rate showed a strong AgNPs dose dependence. The experiments performed with MO and AgNPs (5 mg) in absence of $NaBH_4$ showed no change in absorbance. This clearly indicates that AgNPs have an influence on degradation of MO by $NaBH_4$. The observed rate enhancement by the AgNPs may be attributed to high specific surface area and high reactive activity. The large specific surface area of AgNPs helps effective adsorption of MO which enhances

its reactive activity. The above results clearly suggest that the presence of biosynthesized AgNPs enhance the degradation of MO by $NaHB_4$ and can be used as catalyst in degradation of methyl orange dye by $NaHB_4$.

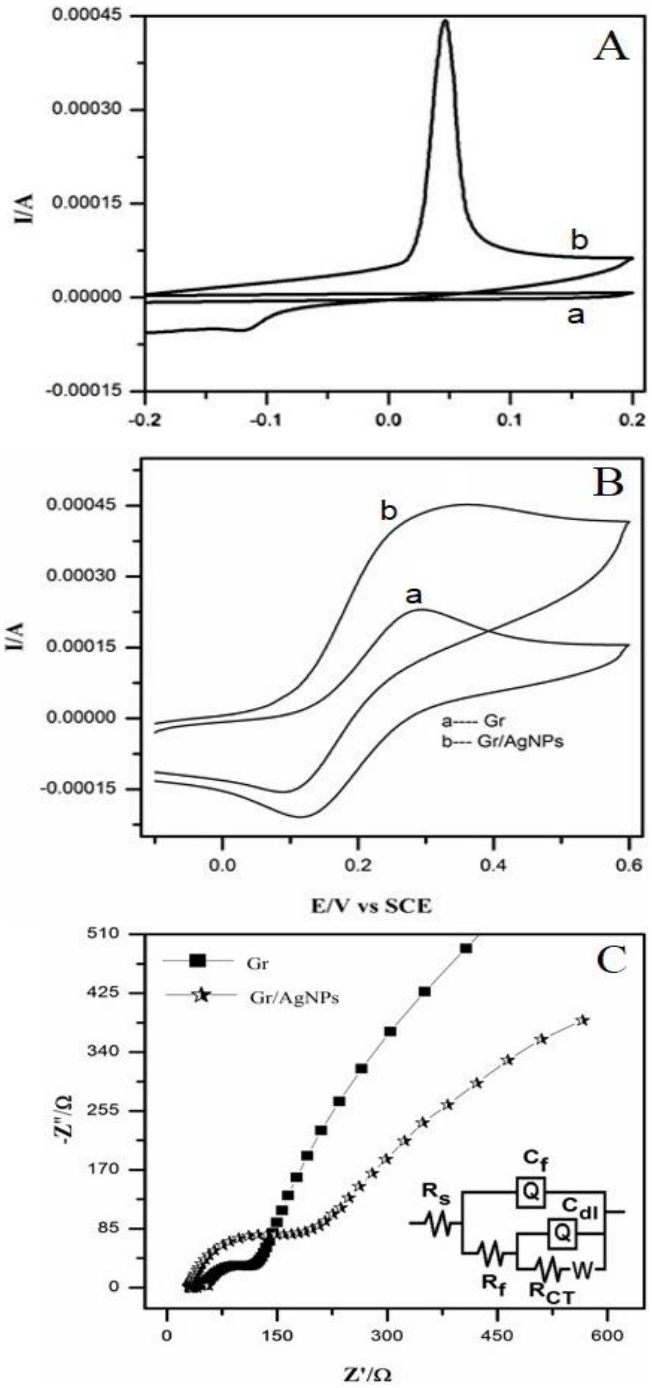

Fig. 4.(A) Cyclic voltammogram of (a) bare Gr electrode (b) and modified Gr/AgNPs electrode in PBS, (B) Cyclic voltammograms of 5 mM $Fe(CN)_6^{3-/4-}$ solution obtained at (a) bare Gr electrode and (b) modified Gr/AgNPs electrode. (C) Impedance spectrum of bare Gr/AgNPs and Gr electrodes in 5 mM $Fe(CN)_6^{3-/4-}$ solution.

Electrocatalytic activity of AgNPs modified Gr electrode

The biosynthesized AgNPs is adsorbed onto Gr electrode by drop casting technique. The adsorption and stability of AgNPs on Gr electrode is confirmed by cyclic voltammetric study of bare Gr and modified Gr/AgNPs electrode in potential range of -0.2 V and +0.2 V Vs. SCE in PBS solution (pH 7.0) at scan rate of 50 mV/s. Cyclic voltammogram of bare Gr electrode showed a poor current response with no oxidation or reduction peak. Contrary to this, modified Gr/AgNPs electrode showed an improved current response with a very prominent oxidation peak at + 0.04 V and an anodic peak current of 0.44 mA (**Fig. 4A**). The peak at +0.04 V is a characteristic of silver nanoparticles and it confirms the adsorption of AgNPs on Gr surface. The results also show that modified Gr/AgNPs electrode has better conductivity compared to bare Gr electrode.

The electrocatalytic properties of bare Gr and modified Gr/AgNPs electrodes are investigated by cyclic voltammetric method using $Fe(CN)_6^{3-/4-}$ as electrochemical redox probe. CV of bare Gr in 5 mM $Fe(CN)_6^{3-/4-}$ shows quasi-reversible redox peaks with a peak separation of 436 mV (**Fig. 4B**). The modified Gr/AgNPs electrode shows increased peak separation (602 mV) and enhanced anodic and cathodic peak currents. The enhanced peak currents correspond to enhanced electrocatalytic activity attributed to AgNPs.

Table 3. EIS data of bare Gr and modified Gr/AgNPs electrode in 5 mM $Fe(CN)_6^{3-/4-}$ solution.

Electrode material	R_s (Ω)	Q_1 ($mFcm^{-2}$)	n_1	R_{ct} (Ω)	Q_2 ($mFcm^{-2}$)	n_2	R_f (Ω)	W (Ω)
Bare Gr	46.12	0.472	0.6	556.2	1.0	1	0.122	1.23
Gr/Ag	41.33	0.009	0.8	265.8	2.6	0.7	0.001	0.11

EIS is a powerful characterization tool for investigating charge transfer processes at electrode/electrolyte interface. The results of EIS studies on bare Gr and modified Gr/AgNPs electrode carried out using 5 mM $Fe(CN)_6^{3-/4-}$ as redox probe are shown in **Fig. 4C** in the form of Nyquist plot and Randles equivalent circuit (inset). Randles equivalent circuit is used to fit the experimental data. Various impedance parameters such as solution resistance (R_s), Faradic resistance (R_f), charge transfer resistance (R_{ct}), Warburg impedance (W), number of electrons transferred (n) and the charge (Q) values obtained by fitting above model circuit are summarized in the **Table 3**. The charge transfer resistance (R_{ct}) value for modified Gr/AgNPs electrode is much less compared to bare Gr electrode suggesting that very fast electron transfer occur for the $Fe(CN)_6^{3-/4-}$ reaction on Gr/AgNPs surface. The values of other parameters also compliment this data there by indicating high conductivity and electrocatalytic activity exhibited due to AgNPs adsorbed on electrode surface.

Phenol remediation studies

Phenols removal from aqueous solutions is investigated by mixing varying amounts 0, 10, 20, 30, 40 and 50 mg of bio-synthesized AgNPs to 50 mL of 20 ppm 2, 4-DCP solution. The residual 2, 4-DCP concentrations after 12 hours of reaction are measured and are shown in **Fig. 5**. The results show a reduction in the initial concentration of 2, 4-DCP from 20 ppm to 18.33, 14.57, 7.58, 5.68 and 4.25 ppm for the respective additions of 10, 20, 30, 40 and 50 mg of AgNPs.

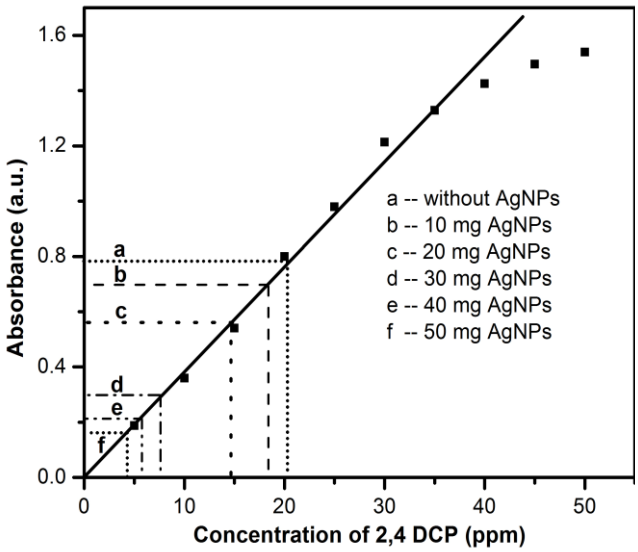

Fig. 5. Removal of 2, 4-dichlorophenol from synthetic solution at different concentration of AgNPs.

The mechanism of action of AgNPs on phenolic compounds is purely governed by electrostatic interactions. It is reported that the charge of AgNPs is defined by the pH of the medium. AgNPs acquire positive, negative and neutral charge respectively under acidic, basic and neutral pH conditions [**32**]. 2, 4-DCP is mildly acidic (p^{Ka} = 7.40) in aqueous solution. As a result, AgNPs acquire positive charge on addition to 2, 4-DCP solution which electrostatically interact with electron cloud on oxygen atom of -OH group of 2, 4-DCP. This results in the adsorption of 2, 4-DCP onto AgNPs surface. This proposed mechanism is equally valid for all substituted phenols. Therefore, it can be concluded that biosynthesized AgNPs can be employed in treatment of phenols from aqueous solutions.

Conclusion

The present study has shown that AgNPs in the size range of 10-11 nm can be effectively synthesized using *Convolvulus pluricaulis* plant extract. The biosynthesized AgNPs are thermally stable upto 200 ^{0}C and exhibited phenol removal, catalytic and electrocatalytic properties. The experimental results demonstrated effective removal of 2, 4- DCP from synthetic solution. The AgNPs have shown excellent enhancement in $NaBH_4$ reduction of MO suggesting their possible application in discoloration of waste water from the dye industry. The biosynthesized AgNPs fabricated on Gr electrode showed high stability and excellent electrocatalytic behavior thus indicating their possible usage for sensing applications.

Acknowledgements

The authors gratefully acknowledge the financial support from Department of Atomic Energy-Board of Research in Nuclear Sciences, BARC, Government of India.

Reference

1. Ren, X.; Chen, C.; Nagatsu, M.; Wang, X.; *Chem. Eng. J.*, **2011**, *170*, 395.
2. Geszke-Moritz, M.; Moritz, M.; *Mater. Sci. Eng. C*, **2013**, *33*, 1008.
3. Moritz, M. *J. Solid State Chem.*, **2011**, *184*, 1761.
4. Caminade, A. M.; Majoral, J. P.; *Acc. Chem. Res.*, **2004**, *37*, 341.
5. Sigot, V.; Arndt-Jovin, D. J.; Jovin, T. M.; *Bioconjugate Chem.*, **2010**, *21*, 1465.
6. Gan, T.; Hu, S.; *Microchim Acta*, **2011**, *175*, 1.
7. Prombutara, P.; Kulwatthanasal, Y.; Supaka, N.; Sramala, I.; Chareonpornwattana, S. *Food Control*, **2012**, *24*, 184.
8. Andelman, T.; Gordonov, S.; Busto, G.; Moghe, P. V.; Riman, R. E. *Nanoscale Res Lett*, **2010**, *5*, 263.
9. Kruszynska, M.; Borchert, H.; Parisi, J.; Kolny-Olesiak, J. *J. Am. Chem. Soc.*, **2010**, *132*, 15976.
10. Chen, C. H.; Tsao, T. C.; Li, W. Y.; Shen, W. C.; Cheng, C. W.; Tang, J. L.; Wu, W. T.; *Microsyst Technol*, **2010**, *16*, 1207.
11. Ning, J.; Men, K.; Xiao, G.; Wang, L.; Dai, Q.; Zou, B.; Zou, G.; *Nanoscale*, **2010**, *2*, 1699.
12. Lee, C. M.; Jeong, H. J.; Lim, S. T.; Sohn, M. H.; Kim, D. W.; *ACS Appl. Mater. Interfaces*, **2010**, *2*, 756.
13. Kanmani, S. S.; Ramachandran, K.; *Renew Energ*, **2012**, *43*, 149.
14. Kim, K. M.; Kang, K. Y.; Kim, S.; Lee, Y. G.; *Curr Appl Phys*, **2012**, *12*, 1199.
15. Wu, X.; Xing, W.; Zhang, L.; Zhuo, S.; Zhou, J.; Wang, G.; Qiao, S.; *Powder Technol.*, **2012**, *224*, 162.
16. Bauer, A.; Hui, R.; Ignaszak, A.; Zhang, J.; Jones, D. J.; *J. Power Sources*, **2012**, *210*, 15.
17. Zhang, F.; Chen, J.; Chen, P.; Sun, Z.; Xu, S.; *AlChE J.*, **2012**, *58*, 1853.
18. Batarseh, K. I.; *J. Antimicrob. Chemother.*, **2004**, *54*, 546.
19. Greenwood, N. N.; Earnshaw, A.; Chemistry of the Elements; Elsevier: Buttrworth-Heinemann Publications, Burlington, **1997**; MA 01803, UK.
20. Pradeep, T.; Anshup; *Thin solid films*, **2009**, *517*, 6441.
21. Reddy, K. R.; Lee, K. P.; Lee, Y.; Gopalan, A. I.; *Mater. Lett.*, **2008**, *62*, 1815.
22. Saha, S.; Pal, A.; Kundu, S.; Basu, S.; Pal, T.; *Langmuir*, **2010**, *26*, 2885-2893.
23. Geoprincy, G.; Srri, B. V.; Poonguzhali, U.; Gandhi, N. N.; Ranganathan, S.; *Asian J Pharm Clini Res*, **2013**, *6*, 8.
24. Patil, R. S.; Kokate, M. R.; Kolekar, S. S.; *Spectrochim Acta A*, **2012**, *91*, 234.
25. Jain D.; Kumar Daima H.; Kachhwaha S.; Kothari S. L.; *Dig J Nanomater Bios*, **2009**, *4*, 557.
26. Shahverdi, A. R.; Fakhimi, A.; Shahverdi, H. R.; Minaian, S.; *Nanomed Nanotech Biol Med*, **2007**, *3*, 168.
27. Shiv Shankar, S.; Ahmad, A.; Sastry, M.; *Biotechnol. Progr.*, **2003**, *19*, 1627.
28. Kumar, P.; Govindaraju, M.; Senthamilselvi, S.; Premkumar, K.; *Colloids Surf., B*, **2013**, *103*, 658.
29. Dubey N. K.; Kumar R.; Tripathi P.; *Curr. Sci*., **2004**, *86*, 37.
30. Agarwal, P.; Sharma, B.; Fatima, A.; Jain, S. K.; *Asian Pac J Trop Biomed*, **2014**, *4*, 245.
31. AL-Asady, A. A. B.; Suker, D. K.; Hassan, K. K.; *J. Med. Plants Res.*, **2014**, *8*, 588.
32. Ravindran, A.; Chandran, P.; Khan, S. S.; *Colloids Surf., B*, **2013**, *105*, 342.

